

# Macroautophagy Involved in Testosterone Synthesis in Leydig Cells of Male Dairy Goats (*Capra Hircus*)

**Hong Chen**

Northwest A&F University: Northwest Agriculture and Forestry University <https://orcid.org/0000-0003-0082-2939>

**Kexin Chen**

Northwest A&F University: Northwest Agriculture and Forestry University

**Fange Zhao**

Northwest A&F University: Northwest Agriculture and Forestry University

**Yihan Guo**

Northwest A&F University: Northwest Agriculture and Forestry University

**Yue Liang**

Northwest A&F University: Northwest Agriculture and Forestry University

**Zhengrong Wang**

Northwest A&F University: Northwest Agriculture and Forestry University

**Tengfei Liu**

Northwest A&F University: Northwest Agriculture and Forestry University

**Shulin Chen** (✉ [csl\\_1359@163.com](mailto:csl_1359@163.com))

Northwest A&F University: Northwest Agriculture and Forestry University

---

## Research

**Keywords:** leydig cells, ultrastructure, testosterone, autophagy, dairy goat

**Posted Date:** June 1st, 2021

**DOI:** <https://doi.org/10.21203/rs.3.rs-559990/v1>

**License:** © ⓘ This work is licensed under a Creative Commons Attribution 4.0 International License.

[Read Full License](#)

---

**Version of Record:** A version of this preprint was published at Theriogenology on December 1st, 2021.  
See the published version at <https://doi.org/10.1016/j.theriogenology.2021.12.023>.

# Abstract

## Background

Testosterone is an important steroid hormone that is indispensable for male sexual development and the reproductive system. Leydig cells (LCs), where autophagy extremely active, reside in the testicular interstitium and are the major sites of testosterone production. However, the ultrastructural characteristics and the functional role of autophagy in LCs of livestock remain unknown. This study was to investigate the role of autophagy in LCs testosterone synthesis of dairy goats at juvenile, pubertal, and adult stages.

## Results

In the present study, morphological results showed that the steroidogenic activity and ultrastructure of the LCs were altered with increasing age. Serum luteinizing hormone and testosterone levels were significantly elevated with sexual maturation. Organelles involved in testosterone synthesis, e.g., smooth endoplasmic reticulum, mitochondria, and lipid droplets, were abundantly distributed within the cytoplasm of LCs in adult testes. However, further studies demonstrated that selective autophagy (including lipophagy and mitophagy) did not participate in the synthesis of testosterone in LCs. In contrast, the autophagy activity was enhanced in the testes at puberty and adulthood compared to that at the juvenile stage. Moreover, a number of different autophagosomes, including phagophores and autolysosomes, were observed within the cytoplasm of LCs.

## Conclusions

Together, our results reveal that macroautophagy is involved in testosterone synthesis mainly through degrading mitochondria and endoplasmic reticulum in the LCs of dairy goats.

## Background

The adult male testis has two important roles within reproduction and physiology, the production of spermatozoa and the secretion of sexual steroids [1]. Spermatogenesis is an extremely complex process that occurs within the seminiferous tubules of the testis. However, Leydig cells (LCs), residing in the testicular interstitium, are the primary location of androgen hormone production [2]. As an important male hormone, testosterone is essential for male sexual development and characteristic maintenance [3]. Serum deficiency of testosterone usually causes male sexual dysfunction and reduced reproductive capacity [4]. Moreover, studies have shown that late-onset hypogonadism symptoms, including erectile dysfunction, diabetes, decrease in bone mineral density, cardiovascular disease, and sleep disturbance, are associated with testosterone decrease in serum [5–7]. During the development of mammals from infancy to adulthood, there are four distinct development stages of LCs, including stem LCs, progenitor LCs, immature LCs, and adult LCs [8]. Testosterone production gradually increases to high levels with the

development of the adult LCs from stem cells of the neonatal testis. Once formed, the adult LCs rarely turn over or die [2].

Current understanding of LC function and its regulation has showed that declines in testosterone production occur with aging and diseases, resulting in hypogonadism and accompanying metabolic changes [2]. In aged rat LCs, autophagy deficiency is indicated to be related to steroidogenic decline [9]. Till date, growing evidence supports the notion that autophagy plays an important role in regulating testosterone synthesis in LCs. This process is initiated in progenitor LCs, peaks in adult LCs, and attenuates in aged LCs [10–13]. It is well established that the production of testosterone in LCs is dependent on luteinizing hormone (LH) stimulation through the hypothalamic-pituitary-testicular axis [14]. Several enzymes are involved in the production of testosterone in LCs, such as the steroidogenic acute regulatory protein (StAR), cholesterol side-chain cleavage enzyme (P450<sub>scc</sub>), and 3 $\beta$ -hydroxysteroid dehydrogenase (3 $\beta$ -HSD) [15]. The functional forms of StAR and P450<sub>scc</sub> are localized in the mitochondrial membrane, and their function is closely related to cholesterol transport. Furthermore, the StAR protein is an important and rate-limiting enzyme in the regulation of testosterone biosynthesis [16]. As steroidogenic cells are capable of storing only very small amounts of hormone, rapid hormone synthesis requires the mobilization of the precursor cholesterol [17]. Recent studies have identified that intracellular lipid droplets are an important source of free cholesterol, and lipophagy contributes to testosterone biosynthesis in rodent LCs [18, 19].

Autophagy is an intracellular lysosomal degradation pathway that eliminates organelles and proteins. The degradation of autophagosome contents is an energy-providing and recycling process [20]. The microtubule-associated protein light chain 3 (LC3) and sequestosome 1 (p62, SQSTM1) biomarkers are widely used for monitoring autophagy [21]. ATG7 is an important member of the autophagy-related gene family that encodes the E1-like enzymes, which facilitate both LC3 and other ATGs [22]. The LC is characterized by large amounts of smooth endoplasmic reticulum and mitochondria, mainly contributing to testosterone biosynthesis. Previous studies have demonstrated that autophagy is extremely active in LCs [13, 23]. Most of these studies were performed on human or rodent LCs; however, the role of autophagy in livestock LCs remains largely unknown. The dairy goat (*Capra hircus*) is one of the most economically useful domestic animals in China. As an important breeding animal, it is necessary to study the regulation mechanism of reproductive capacity in males. The objectives of the current study were to analyze the morphological characteristics of LCs during postpartum development and to explore the role of autophagy in testosterone biosynthesis in dairy goats.

## Methods

### Animals

The dairy goat is one of the most economically useful animals widely distributed in the Shaanxi Province of China. In the present study, we used dairy goats of different ages to represent three major developmental stages of the testes: 3 months of age (juvenile), 6 months of age (puberty), and 24

months of age (adult). A total of nine dairy goats were used in this experiment. After anaesthetization of the dairy goats by intramuscular administration of pentobarbital sodium, samples of the testes were collected immediately and fixed for further analysis.

## Chemical Reagents

The following antibodies and reagents were used: Oil red O solution (Sigma, O0625), rabbit 3 $\beta$ -HSD antibody (ABclonal, A19266), rabbit ATG 7 antibody (ABclonal, A0691), Alexa Fluor 488 conjugated rabbit anti-LC3 antibody (CST, 13082), rabbit anti-LC3A/B (CST, 12741), rabbit anti-SQSTM1/p62 (CST, 5114), rabbit anti-PINK1 antibody (ABclonal, A11435), rabbit anti-Parkin antibody (ABclonal, A0968), rabbit anti- $\beta$ -actin (Bioworld, AP0060), BODIPY 493/503 (Invitrogen, D3922), Anti-rabbit secondary antibody (Alexa Fluor® 594 Conjugate) and Anti-rabbit secondary antibody (Alexa Fluor® 488 Conjugate) were purchased from Cell Signaling Technology. Goat Testosterone Elisa Kit (Shanghai Enzyme Link Biotechnology Co., Ltd. China). Goat Luteinizing Hormone (LH) Elisa Kit (Shanghai Enzyme Link Biotechnology Co., Ltd. China). DAB kit (Boster Bio-Technology, Wuhan, China).

## Light microscopy

The dairy goat testes samples were fixed in 10% neutral buffered formalin (v/v) overnight, and then the samples were embedded in paraffin and sectioned serially (5  $\mu$ m). The sample sections were stained with hematoxylin and eosin for observation by light microscopy (Olympus DP73, Tokyo, Japan).

## Oil red O staining

Tissue sections were collected from frozen samples of the testes of dairy goats. The frozen sections were washed with phosphate-buffered saline (PBS), fixed with 4% formaldehyde for 10 min, and stained with fresh Oil red O solution (Oil O-saturated solution in isopropanol:water, 3:2) for 15 min. Then, the sections were washed with 60% isopropanol (v/v) to remove background staining. Finally, stained frozen sections of the testes were imaged using light microscopy (Olympus DP73, Tokyo, Japan).

## Immunohistochemistry (IHC)

The tissue sections of the testes were deparaffinized in xylene and rehydrated in a graded series of alcohol. After washing briefly in PBS solution, the sections were placed in 3% hydrogen peroxide for 10 min to eliminate endogenous peroxidase activity. The sections were then boiled for 15 min in sodium citrate buffer for antigen retrieval. The sections were chilled at room temperature and then blocked with 5% bovine serum albumin. The sections were incubated with primary antibodies (3 $\beta$ -HSD antibody or ATG7 antibody) overnight at 4°C. After washing with PBS three times for 5 min each, the sections were incubated with the secondary antibody diluted at 1:200 for 1 h at room temperature. The sections were washed thrice with PBS, and the positive reaction was visualized using a DAB kit. The sections incubated with PBS alone served as the negative control.

## Immunofluorescence staining

Sections of the frozen testes of dairy goats were fixed and then incubated overnight at 4°C with Alexa Fluor 488-conjugated rabbit anti-LC3 antibody. After washing with PBS three times for 5 min each, the testes sections were stained with DAPI to highlight the nuclei. Stained sections were observed using fluorescent microscopy. For the immunofluorescence double-labeling, the frozen testes sections were incubated overnight at 4°C with rabbit anti-LC3A/B antibody. The sections were then incubated with the corresponding fluorescent secondary antibody for 1 h at 37°C. After washing thrice with PBS, the sections were stained with BODIPY 493/503 for 15 min. The stained sections were observed under a confocal microscope.

## **Transmission electron microscopy (TEM)**

The testes tissue samples from dairy goats were fixed in 2.5% (v/v) glutaraldehyde in PBS (4°C, pH 7.4) for 24 h. After rinsing in PBS, the samples were fixed in 1% (w/v) osmium tetroxide for 1 h at 37°C and washed again with PBS. Subsequently, the testes samples were dehydrated in ascending concentrations of alcohol, infiltrated with a propylene oxide-Araldite mixture (50% propylene oxide: Araldite), and then embedded in Araldite. Ultrathin sections (50 nm) were first stained with uranyl acetate, and then stained with lead citrate. The electron micrographs were obtained using a transmission electron microscope (Hitachi H-7650, Japan).

## **Hormone assay**

After the dairy goats were anesthetized, blood was collected via jugular vein puncture. Serum was isolated by centrifugation at  $1200 \times g$  for 20 min and stored at -80°C until analysis. The concentrations of testosterone and LH in the serum were determined in duplicate using an enzyme-linked immunosorbent assay (ELISA) kit according to the manufacturer's instructions.

## **Quantitative polymerase chain reactions analyses (qPCR)**

Total RNA was extracted from the testes samples of the dairy goats using the Trizol reagent according to the manufacturer's instructions. After the RNA concentration was measured, cDNA was synthesized using the Prime Script reverse transcription reagent kit (Takara Bio Inc.). qPCR was performed using a Light Cycler detection system (Roche), and the samples for qPCR were prepared using SYBR green super mix (Bio-Rad Laboratories). All values were normalized to those of  $\beta$ -actin to balance potential irregularities in the RNA concentration. The  $2^{-\Delta\Delta C_t}$  method was used to calculate fold changes in gene expression (Table 1).

Table 1  
The qPCR primer sequences used in the present study.

Gene Name	Primers	
	Forward	Reverse
StAR	GGAAGGGATGCCAGTCACAAGATG	CTGCGAGAGGACCTGATTGATGATG
CYP11A1	CAGGCTGAATGTTTGGTTTGAAGAAG	AGGAGGAGGAGAGGAGGAAGTAGG
3 $\beta$ -HSD	CTATGTTGGCAATGTGGC	ATCTCGCTGAGCTTTCTTAT
17 $\beta$ 1-HSD	GATCCCTGGGTCAAGTAGGAAATGC	AGGTGCGTATATGTGTGCTCAGTTG
$\beta$ -actin	CTGAGCGCAAGTACTCCGTGT	GCATTTGCGGTGGACGAT

## Western blotting

The testes samples were harvested from the goats at different development stages and homogenized in cold RIPA-like buffer (Sigma) and supplemented with a protein inhibitor on ice. The homogenates were centrifuged at 12,000  $\times g$  for 15 min, and the protein concentrations were determined using a protein assay from Bio-Rad Laboratories. The lysates containing equal amounts of proteins were separated on a 10% gradient SDS-PAGE gel and transferred onto a PVDF membrane. Nonspecific binding was blocked using 5% nonfat milk in Tris-buffered saline with Tween 20 (TBST) for 1 h at room temperature. Next, the membranes were incubated overnight at 4°C with primary antibodies and  $\beta$ -actin antibody. After washing with TBST three times for 5 min each, the membranes were incubated with peroxidase-linked secondary antibody for 1 h at room temperature. Protein bands were scanned using an ECL detection system (Vazyme Biotech, China) and immunoreactive bands were quantified using Quantity One software (Bio-Rad Laboratories).

## Statistical analysis

All data are presented as the means  $\pm$  SEM. The statistical significance of the difference between the mean values for the different groups was measured by ANOVA with the Multiple Comparison Test using GraphPad Prism 7.0 software. All the quantification data were repeated triply and the data were considered significant when the *p-value* was less than 0.05 (\*) or 0.01 (\*\*).

## Results

### Characteristics of LCs in dairy goats of different ages

In the present study, the testes of the dairy goats at three different ages were analyzed: juvenile (3 months of age), puberty (6 months of age), and adult (24 months of age). During the juvenile stage (Fig. 1A and D), testicular spermatogenesis did not occur. The seminiferous epithelium was thin and mainly comprised of spermatogonia. Clusters of LCs could be observed in the interstitial spaces between seminiferous tubules and were usually arranged around blood vessels of varying diameters. At puberty

(Fig. 1B and E) and adulthood (Fig. 1C and F), spermatogenesis was active, and the seminiferous tubules were lined with a continuous germinal epithelium consisting of mainly developing germ cells. With sexual maturation, the diameter and area of the seminiferous tubules increased noticeably (Fig. 1-Data1). Conversely, a marked decrease in the number of LCs was observed in the longitudinal section of testicular tissue at the adult stage compared with that at the juvenile stage (Fig. 1-Data2). Furthermore, IHC analysis was performed to detect the expression of  $3\beta$ -HSD, a key enzyme involved in the biosynthesis of steroid hormones, in the testes of the dairy goats (Fig. 1H-J). The immunopositive reaction of  $3\beta$ -HSD mainly appeared in the cytoplasm of LC close to the nucleus. Its weak to moderate labeling was observed from the juvenile (Fig. 1H and K) to pubertal (Fig. 1I and L) stages, whereas moderate to intense immunosignals occurred in the testes at the adult stage (Fig. 1J and M, Data3). Moreover, some immunopositive signals of  $3\beta$ -HSD were adjacent to the surface of the seminiferous tubule at the adult stage of the dairy goat (Fig. 1M).

The hypothalamic-pituitary axis is integrally involved in the regulation of testicular testosterone production. The LH secreted by the pituitary is essential for regulating the levels of the proteins and enzymes involved in steroidogenesis in LCs. In the present study, ELISA results showed that serum levels of LH in dairy goats increased with age (Fig. 2-Data1). The highest value was found at the adult stage. There was also an increase in serum testosterone levels with age of the dairy goats (Fig. 2-Data2). Differences among the different age groups were significant ( $p < 0.01$ ). Consistent with these results, the mRNA levels of proteins and enzymes associated with steroidogenesis were significantly higher at the adult stage than at the juvenile stage (Fig. 2-Data3). Oil red O staining results indicated a small amount of lipid droplets within the LCs at the juvenile stage, whereas a large amount of lipid droplets was observed at the pubertal and adult stages (Fig. 2A ~ C, Data4). Moreover, TEM was used to observe the ultrastructural characteristics of LCs. Results showed that the LCs displayed a round eccentric nucleus with prominent nucleoli at the juvenile stage (Fig. 2D). At the perinuclear cytoplasm, the vesicular endoplasmic reticulum was dispersed and in contact with the mitochondria; in addition, several lipid droplets were scattered in the cytoplasm (Fig. 2G). At the pubertal and adult stages (Fig. 2E and F), the LC nucleus appeared in an oval shape with irregular membranes. The diameter of the nucleus decreased with the age of dairy goats (Fig. 2-Data5). However, strikingly, the predominant organelles (smooth endoplasmic reticulum, mitochondria, and lipid droplets) were abundantly dispersed in the LC cytoplasm (Fig. 2H and I). Especially, the number and size of lipid droplets within LCs were markedly increased at the adult stage (Fig. 2-Data6 and Data7).

## **Lipophagy is not involved in testosterone synthesis in the LCs of dairy goats**

The biosynthesis of steroid hormones starts from the common precursor, free cholesterol, which can be synthesized *de novo* from acetate and stored in lipid droplets, or originate from LC membranes. As indicated above, there were numerous lipid droplets in LCs of the adult dairy goats. Therefore, we speculated that autophagy might be involved in testosterone synthesis via lipid metabolism in LCs. To test this hypothesis, we examined the expression of ATG7 in the testes of dairy goats of different ages.

The IHC results showed that the immunopositive reaction of ATG7 mainly appeared in the cytoplasm of LCs (Fig. 3A-D). Furthermore, intense immunosignals were observed at the pubertal and adult stages (Fig. 3-Data1). The immunofluorescence analysis of LC3 also showed increases in punctate immunosignals (representing autophagosomes) in LCs at both puberty and adulthood (Fig. 3F-K). However, further analysis using confocal microscopy indicated that the majority of LC3-II puncta were unassociated with lipid droplets in the LCs (Fig. 3L-T). Consistent with the results of confocal microscopy, TEM results showed the disappearance of the phagophore (pre-autophagosome) around the lipid droplet, and the structure of the lipophagic vesicle in the LC was rarely observed (Fig. 3U-W). Based on these results, we conclude that autophagy is highly active in pubertal and adult LCs of the dairy goat, whereas lipophagy is not involved in steroidogenesis.

## **Macroautophagy might regulate steroidogenesis in LCs of dairy goats**

The levels of autophagy markers (ATG7, LC3, and p62/SQSTM1) of LCs were analyzed using western blotting. Consistent with the IHC results, the relative protein level of ATG7 was high in adult testes (Fig. 4A, Data1). Autophagy activity was assessed by measuring LC3 conservation and p62 degradation. Western blot analysis detected markedly higher LC3-II conversion in the pubertal and adult testes than in the juvenile testes (Fig. 4A, Data2). Moreover, a dramatically elevated degradation of p62 was also observed (Fig. 4A, Data3). To further investigate whether mitophagy is involved in steroidogenesis in LCs, we assessed the protein levels of Parkin and Pink1 (specific markers of mitophagy) in the testes of the dairy goats at different ages. Immunoblotting results showed the relative low protein levels of the two markers of mitophagy in the testes all age groups (Fig. 4A, Data4). Additionally, the autophagosomes were further confirmed by TEM. The autophagosomes, that typically have a double membrane, were easily detected in LC at puberty and adulthood (Fig. 4B). After sequestration of portions of the cytoplasm, the content of the autophagosomes and its bordering membrane remained morphologically unchanged, and sometimes, the sequestered mitochondrion and endoplasmic reticulum were easily recognized (Fig. 4B-c and f). Degradative autolysosomes, typically with one limiting membrane, were also observed in LCs (Fig. 4B-e). Thus, these results suggest that macroautophagy in LCs of dairy goats might be involved in the synthesis of testosterone.

## **Discussion**

The steroid-secreting LC regulates the development and activity of the male reproductive tract and external sex characteristics and enhances spermatogenesis in the seminiferous tubules [24, 25]. In mammals, the LCs progressively improve their capacity to synthesize testosterone during development and differentiation from stem LCs to the adult LCs, with production peaking in the adult LCs [2]. In the adult testes, LCs show morphological characteristics such as abundant smooth endoplasmic reticulum, numerous mitochondria, and a variable number of lipid droplets [26]. However, most of the research to date has been on mouse LCs, whereas the ultrastructural characteristics and the mechanism of testosterone synthesis in livestock LCs have not been well elucidated. In the current study, we used dairy

goats as experimental animals to observe the ultrastructure of LCs at different ages. Our results suggested that the number and area of LCs in each longitudinal testicular section decreased from the juvenile to adult stages. The positive reaction of 3 $\beta$ -HSD mainly appeared in the cytoplasm of LCs and close to the nucleus. Its weak to moderate reaction was observed from the juvenile to pubertal testes, whereas intense immunopositive signals were present in adult testes. Moreover, TEM results indicated that at the juvenile stage, the LCs displayed a round eccentric nucleus, and the vesicular endoplasmic reticulum and several mitochondria were present in the cytoplasm. At the pubertal and adult stages, the nucleus of the LC showed an oval shape with irregular membranes. Well-developed smooth endoplasmic reticulum and mitochondria were abundantly dispersed in the cytoplasm, and numerous lipid droplets were also observed. All the morphological alterations observed in the present study could be related to an enhancement of testosterone synthesis with sexual maturation in dairy goat LCs. The production of testosterone in LCs is dependent on LH stimulation through the hypothalamic-pituitary-testicular axis [14]. In the current study, ELISA results showed an obvious increase in serum levels of LH at the pubertal and adult stages compared with that at the juvenile stage. Responding to the LH stimulation, the serum levels of testosterone and the mRNA levels of related enzymes were also increased considerably. Wing and Ewing [27] reported that in response to LH infused into the testes, testosterone could be synthesized at high levels for several hours. A positive correlation was observed between the ability of LCs to produce testosterone and the content of smooth endoplasmic reticulum [28]. Thus, it could be suggested that LH regulates not only the ability of steroidogenesis but also LC ultrastructure.

Intracellular free cholesterol serves as the initial substrate for testosterone synthesis, and it is usually stored in cytoplasmic lipid droplets in the form of cholesterol esters in LCs [25, 29]. In hepatocytes, the participation of autophagy in cellular lipid droplets metabolism has been indicated [30]. Previous studies have reported that lipophagy contributes to testosterone biosynthesis in LCs [18, 31]. However, Gao et al., [12] reported that in autophagy-deficient LCs, the content of cellular lipid droplets clearly decreased compared with that in the control group. Their further investigations indicated a novel functional role for autophagy in cholesterol uptake. Nevertheless, LCs indeed exhibit higher levels of autophagy than other cells [13]. In order to investigate the potential roles of autophagy in testosterone synthesis by LCs of the dairy goat, we observed the correlation between LC3 and lipid droplets. In this study, confocal microscopy analyses and TEM results showed that lipid droplets were not enveloped by autophagosomes. Moreover, immunoblotting detected low levels of Parkin and PINK1 in the adult testes of dairy goats. Thus, the above results indicate that selective autophagy (including lipophagy and mitophagy) was not involved in the synthesis of testosterone in LCs of dairy goats. As an important intracellular lysosomal degradation pathway, autophagy can eliminate organelles and proteins to produce basal metabolic substances, which are then exported back to the cytoplasm for fresh synthesis of macromolecules [32]. The results of immunofluorescence and immunoblotting demonstrated that the levels of specific autophagic markers were higher in the LCs at the pubertal and adult stages compared with that at the juvenile stage. Furthermore, autophagosomes (mainly mitochondria and endoplasmic reticulum cargos) were observed under TEM in the pubertal and adult testes. Therefore, it is suggested that the increased levels of

testosterone synthesis are in line with the alteration of macroautophagy activity in the development of dairy goat LCs.

## Conclusions

In conclusion, at different stages of development, the LCs of the dairy goat, *Capra hircus*, showed obvious morphological characteristics including steroidogenic activity (active 3 $\beta$ -HSD), well-developed smooth endoplasmic reticulum, dynamic mitochondria, and lipid droplets. All these morphological changes in LCs were closely related to the ability for testosterone synthesis. Moreover, our present study provides new evidence on the involvement of autophagy in the synthesis of testosterone. This study indicates that macro-autophagy regulates testosterone synthesis in LCs mainly through the breakdown of mitochondria and endoplasmic reticulum in adult dairy goats.

## Abbreviations

LCs: Leydig cells; LH: luteinizing hormone; StAR: steroidogenic acute regulatory protein; P450<sub>scc</sub>: cholesterol side-chain cleavage enzyme; 3 $\beta$ -HSD: 3 $\beta$ -hydroxysteroid dehydrogenase; LC3: microtubule-associated protein light chain 3; p62: sequestosome 1; ATG7: autophagy-related gene 7; BODIPY 493/503: 4,4-difluoro-1,3,5,7,8-pentamethyl-4-bora-3a,4a-diaza-s-indacene; PBS: phosphate buffered saline; Oil red O solution: Oil O-saturated solution in isopropanol; IHC: Immunohistochemistry; DAB: 3,3-N-Diaminobenzidine Tetrahydrochloride; DAPI: 2-(4-Amidinophenyl)-6-indolecarbamide dihydrochloride; TEM: Transmission electron microscopy; ELISA: enzyme-linked immunosorbent assay; qPCR: quantitative polymerase chain reactions analyses; RIPA: radioimmunoprecipitation assay buffer; SDS-PAGE: dodecyl sulfate, sodium salt (SDS)-Polyacrylamide gel electrophoresis; PVDF: polyvinylidene fluoride; TBST: Tris base-phosphate buffered saline plus Tween-20; ECL: electrochemiluminescence

## Declarations

### Ethics approval and consent to participate

Experimental protocols and procedures used in the present experiment were approved by and complied with the guidelines of the Animal Research Institute Committee (Northwest A&F University, Shaanxi, China). All efforts were made to minimize animal suffering and the procedures were approved by the Science and Technology Agency of Shaanxi Province, Approval ID NO. SYXK (SN) 2018-0003.

### Consent for publication

All the authors read and agree to the content of this paper and its publication.

### Availability of data and material

The data analyzed during the current study are available from the corresponding authors on reasonable request.

### Competing interests

The authors declare that they have no competing interests.

### Funding

This work was supported by grants from the National Natural Science Foundation of China (32002242) and the Doctoral Scientific Research Found of Northwest A&F University (2452019202), PR-China.

### Authors' contributions

H. C. designed the experiments and drafted the manuscript. K. C., F. Z., Y. G., Y. L., and Z. W., participated in the study design and analyze the data. Prof. S. Chen and A.P. T. Liu conceived the study and participated in its design and coordination and helped draft the manuscript. All authors reviewed and approved the manuscript.

### Acknowledgments

We would like to thank Life Science Research Core Services (Northwest A&F University, China) for providing us with the transmission electron microscopy and technical guidance.

## References

1. Kumar S, Roy B, Rai U. Hormonal Regulation of Testicular Functions in Reptiles. *Hormones and Reproduction of Vertebrates*. 2011; 2013(16):63-88. <https://doi.org/10.1016/B978-0-12-374930-7.10003-2>.
2. Zirkin BR, Papadopoulos V. Leydig cells: formation, function, and regulation. *Biol Reprod*. 2018; **99**(1):101-111. <https://doi.org/10.1093/biolre/ioy059>.
3. Sinclair M, Grossmann M, Gow PJ, Angus PW. Testosterone in men with advanced liver disease: abnormalities and implications. *J Gastroenterol Hepatol*. 2015; 30(2):244-251. <https://doi.org/10.1111/jgh.12695>.
4. Morales A, Bella AJ, Chun S, Lee J, Assimakopoulos P, Bebb R, et al. A practical guide to diagnosis, management and treatment of testosterone deficiency for Canadian physicians. *Can Urol Assoc J*. 2010; 4(4):269-275. <https://doi.org/10.5489/cuaj.880>.
5. Amano T, Imao T, Takemae K, Iwamoto T, Nakanome M. Testosterone replacement therapy by testosterone ointment relieves lower urinary tract symptoms in late onset hypogonadism patients. *Aging Male*. 2010; 13(4):242-246. <https://doi.org/10.3109/13685538.2010.487552>.
6. Permpongkosol S, Tantirangsee N, Ratana-olarn K. Treatment of 161 men with symptomatic late onset hypogonadism with long-acting parenteral testosterone undecanoate: effects on body

- composition, lipids, and psychosexual complaints. *J Sex Med.* 2010; 7(11):3765-3774.  
<https://doi.org/10.1111/j.1743-6109.2010.01994.x>.
7. Liu ZY, Zhou RY, Lu X, Zeng QS, Wang HQ, Li Z, et al. Identification of late-onset hypogonadism in middle-aged and elderly men from a community of China. *Asian J Androl.* 2016; 18(5):747-753.  
<https://doi.org/10.4103/1008-682X.160883>.
  8. Chen H, Ge RS, Zirkin BR. Leydig cells: From stem cells to aging. *Mol Cell Endocrinol.* 2009; 306(1-2):9-16. <https://doi.org/10.1016/j.mce.2009.01.023>.
  9. Li WR, Chen L, Chang ZJ, Xin H, Liu T, Zhang YQ, et al. Autophagic deficiency is related to steroidogenic decline in aged rat Leydig cells. *Asian J Androl.* 2011, 13(6):881-888.  
<https://doi.org/10.1038/aja.2011.85>.
  10. Selvaraj V, Koganti PP. Eat, drink, and be merry: Leydig cell autophagy in testosterone production. *Biol Reprod.* 2018; 99(6):1113-1115. <https://doi.org/10.1093/biolre/iox153>.
  11. Yang W, Li L, Huang X, Kan G, Lin L, Cheng J, et al. Levels of Leydig cell autophagy regulate the fertility of male naked mole-rats. *Oncotarget.* 2017; 8(58):98677-98690.  
<https://doi.org/10.18632/oncotarget.22088>.
  12. Gao F, Li G, Liu C, Gao H, Wang H, Liu W, et al. Autophagy regulates testosterone synthesis by facilitating cholesterol uptake in Leydig cells. *J Cell Biol.* 2018; 217(6):2103-2119.  
<https://doi.org/10.1083/jcb.201710078>.
  13. Gao H, Liu C, Li W. Assessing Autophagy in the Leydig Cells. *Methods Mol Biol.* 2019; 1854:71-85.  
[https://doi.org/10.1007/7651\\_2018\\_123](https://doi.org/10.1007/7651_2018_123).
  14. Ramaswamy S, Weinbauer GF. Endocrine control of spermatogenesis: Role of FSH and LH/ testosterone. *Spermatogenesis.* 2014; 4(2):e996025.  
<https://doi.org/10.1080/21565562.2014.996025>.
  15. Wang Y, Chen F, Ye L, Zirkin B, Chen H. Steroidogenesis in Leydig cells: effects of aging and environmental factors. *Reproduction.* 2017; 154(4):R111-r122. <https://doi.org/10.1530/REP-17-0064>.
  16. Sasaki G, Zubair M, Ishii T, Mitsui T, Hasegawa T, Auchus RJ. The contribution of serine 194 phosphorylation to steroidogenic acute regulatory protein function. *Mol Endocrinol.* 2014; 28(7):1088-1096. <https://doi.org/10.1210/me.2014-1028>.
  17. Danielsen ET, Moeller ME, Yamanaka N, Ou Q, Laursen JM, Soenderholm C, et al. A Drosophila Genome-Wide screen identifies regulators of steroid hormone production and developmental timing. *Dev Cell.* 2016; 37(6):558-570. <https://doi.org/10.1016/j.devcel.2016.05.015>.
  18. Ma Y, Zhou Y, Zhu YC, Wang SQ, Ping P, Chen XF. Lipophagy contributes to testosterone biosynthesis in male rat Leydig Cells. *Endocrinology.* 2018; 159(2):1119-1129. <https://doi.org/10.1210/en.2017-03020>.
  19. Khawar MB, Liu C, Gao F, Gao H, Liu W, Han T, et al. Sirt1 regulates testosterone biosynthesis in Leydig cells via modulating autophagy. *Protein Cell.* 2021; 12(1):67-75.  
<https://doi.org/10.1007/s13238-020-00771-1>.

20. Kim KH, Lee MS. Autophagy—a key player in cellular and body metabolism. *Nat Rev Endocrinol*. 2014; 10(6):322-337. <https://doi.org/10.1038/nrendo.2014.35>.
21. Yoshii SR, Mizushima N. Monitoring and measuring autophagy. *Int J Mol Sci*. 2017; 18(9). <https://doi.org/10.3390/ijms18091865>.
22. Xie Z, Klionsky DJ. Autophagosome formation: core machinery and adaptations. *Nat Cell Biol*. 2007; 9(10):1102-1109. <https://doi.org/10.1038/ncb1007-1102>.
23. Yi J, Tang XM. Functional implication of autophagy in steroid-secreting cells of the rat. *Anat Rec*. 1995; 242(2):137-146. <https://doi.org/10.1002/ar.1092420202>.
24. Zhou R, Wu J, Liu B, Jiang Y, Chen W, Li J, et al. The roles and mechanisms of Leydig cells and myoid cells in regulating spermatogenesis. *Cell Mol Life Sci*. 2019; 76(14):2681-2695. <https://doi.org/10.1007/s00018-019-03101-9>.
25. Haider SG. Cell biology of Leydig cells in the testis. *Int Rev Cytol*. 2004; 233:181-241. [https://doi.org/10.1016/S0074-7696\(04\)33005-6](https://doi.org/10.1016/S0074-7696(04)33005-6).
26. Saraiva KL, Silva AK, Wanderley MI, De Araújo AA, De Souza JR, Peixoto CA. Chronic treatment with sildenafil stimulates Leydig cell and testosterone secretion. *Int J Exp Pathol*. 2009; 90(4):454-462. <https://doi.org/10.1111/j.1365-2613.2009.00660.x>.
27. Wing TY, Ewing LL, Zirkin BR. Effects of luteinizing hormone withdrawal on Leydig cell smooth endoplasmic reticulum and steroidogenic reactions which convert pregnenolone to testosterone. *Endocrinology*. 1984; 115(6):2290-2296. <https://doi.org/10.1210/endo-115-6-2290>.
28. Wing TY, Ewing LL, Zegeye B, Zirkin BR. Restoration effects of exogenous luteinizing hormone on the testicular steroidogenesis and Leydig cell ultrastructure. *Endocrinology*. 1985; 117(5):1779-1787. <https://doi.org/10.1210/endo-117-5-1779>.
29. Martin S, Parton RG. Lipid droplets: a unified view of a dynamic organelle. *Nat Rev Mol Cell Biol*. 2006; 7(5):373-378. <https://doi.org/10.1038/nrm1912>.
30. Madrigal-Matute J, Cuervo AM. Regulation of liver metabolism by autophagy. *Gastroenterology*. 2016; 150(2):328-339. <https://doi.org/10.1053/j.gastro.2015.09.042>.
31. Tarique I, Vistro WA, Bai X, Yang P, Hong C, Huang Y, et al. LIPOPHAGY: a novel form of steroidogenic activity within the LEYDIG cell during the reproductive cycle of turtle. *Reprod Biol Endocrinol*. 2019; 17(1):19. <https://doi.org/10.1186/s12958-019-0462-2>.
32. Glick D, Barth S, Macleod KF. Autophagy: cellular and molecular mechanisms. *J Pathol*. 2010; 221(1):3-12. <https://doi.org/10.1002/path.2697>.

## Figures

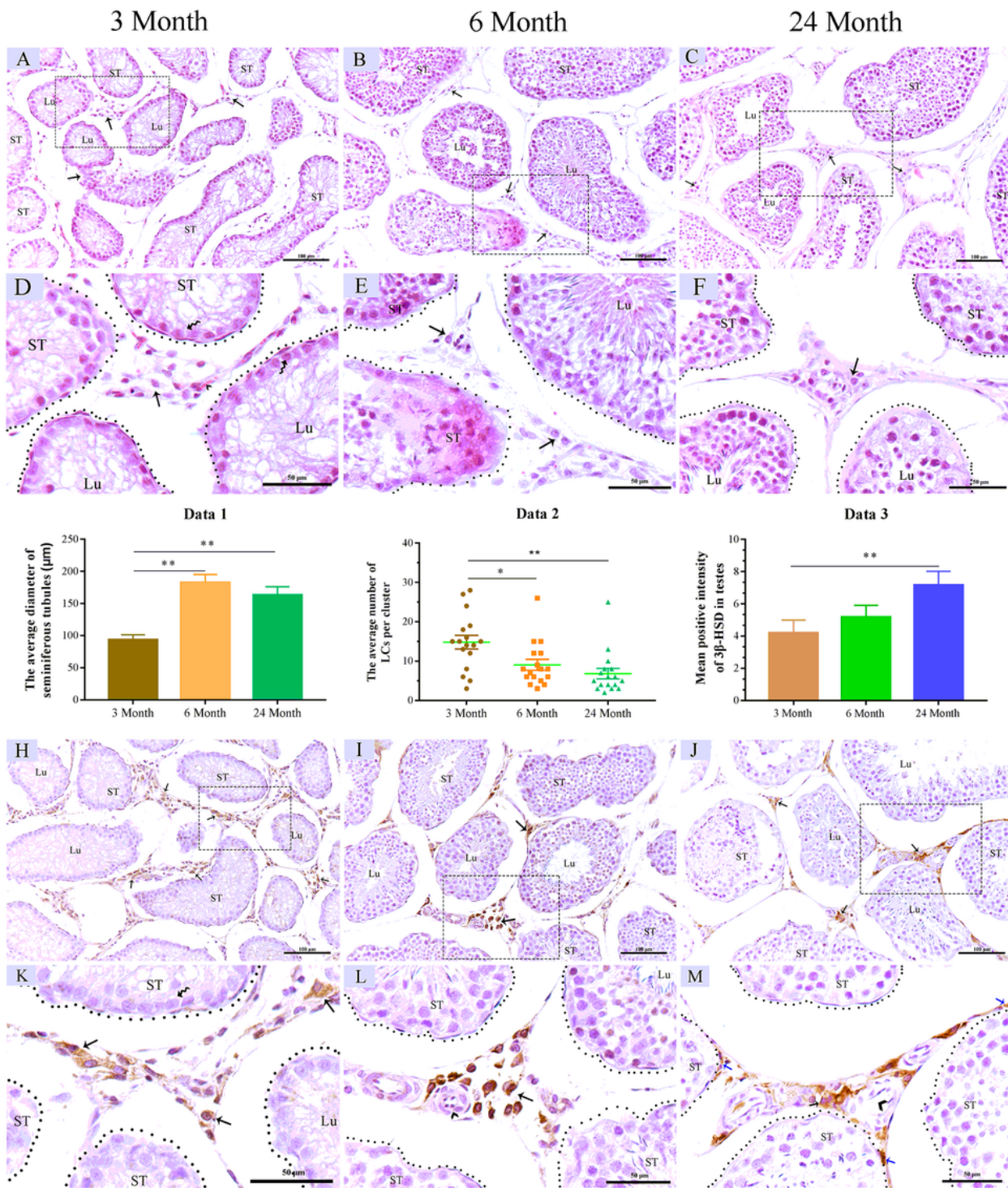


**Figure 1**

Light micrographs of testes tissue from the dairy goats at different ages. The testes tissue sections in juvenile (A), pubertal (B), and adult (C) stages, H&E staining. (D, E, and F) The higher magnification pictures of the corresponding black rectangle in upper panel, respectively. Immunohistochemistry of 3β-HSD in the testes at the juvenile (H), pubertal (I), and adult (J) stages. (K, L, and M) The higher magnification pictures of the corresponding black rectangle in upper panel, respectively. The

quantification of the average diameter of seminiferous tubules (Data 1) and the number of LCs per cluster (Data 2) based on light micrographs. Data 3. The relative mean positive intensity of 3 $\beta$ -HSD in the testes at different stages. Each value represents the mean  $\pm$  SEM, \* $p$  < 0.05, \*\* $p$  < 0.01. ST: seminiferous tubules; Lu: lumen; Curved arrow: spermatogonia; Black arrow: Leydig cells; Black arrowhead: capillary; Scale bar: A, B, C, H, I, and J = 100  $\mu$ m; D, E, F, K, L, and M = 50  $\mu$ m.

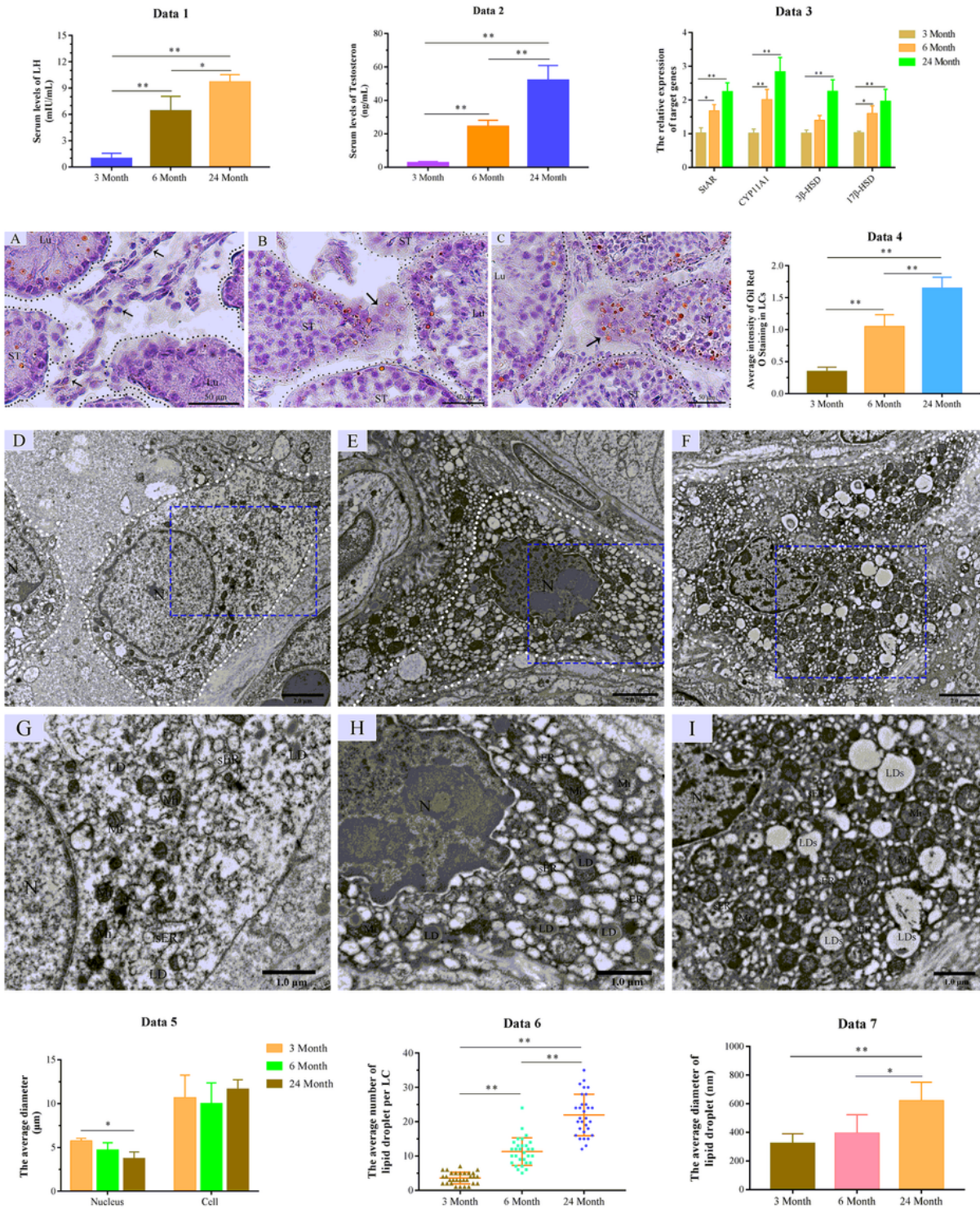
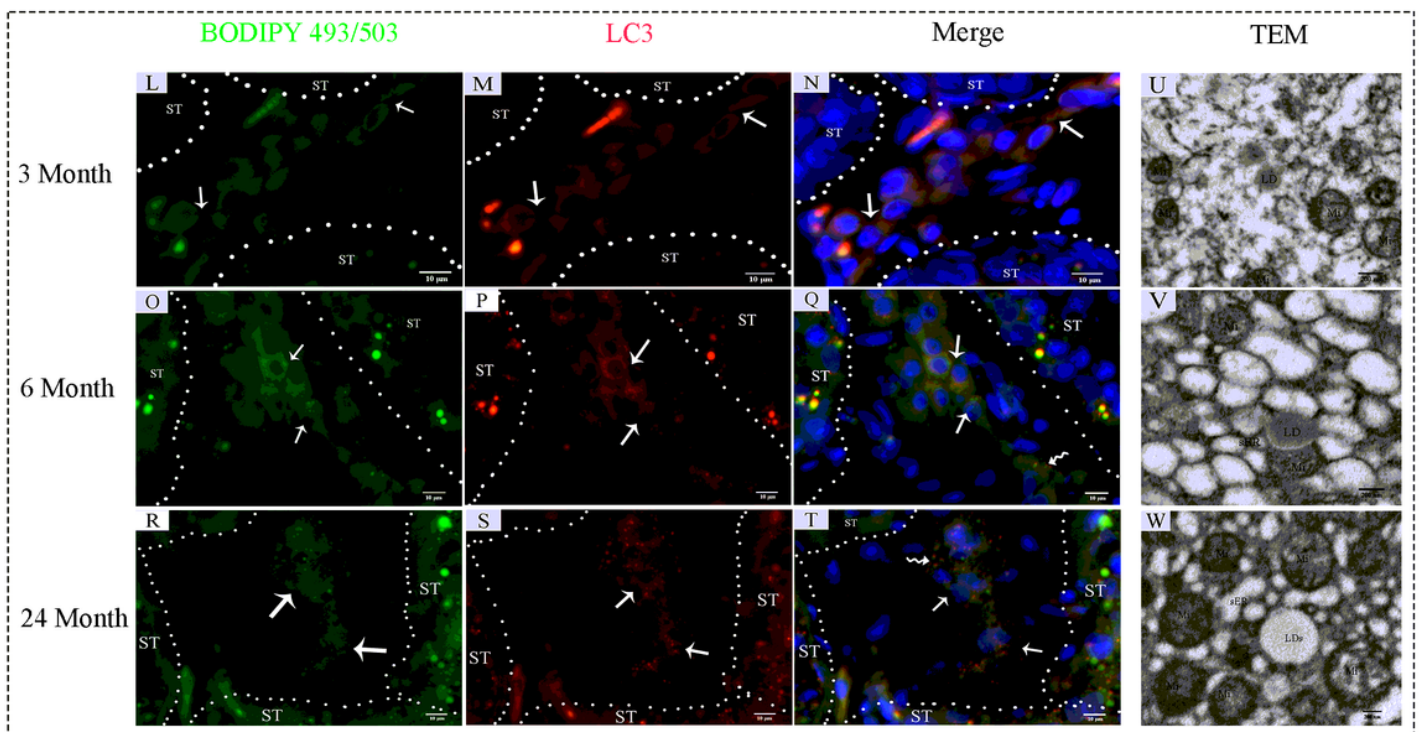
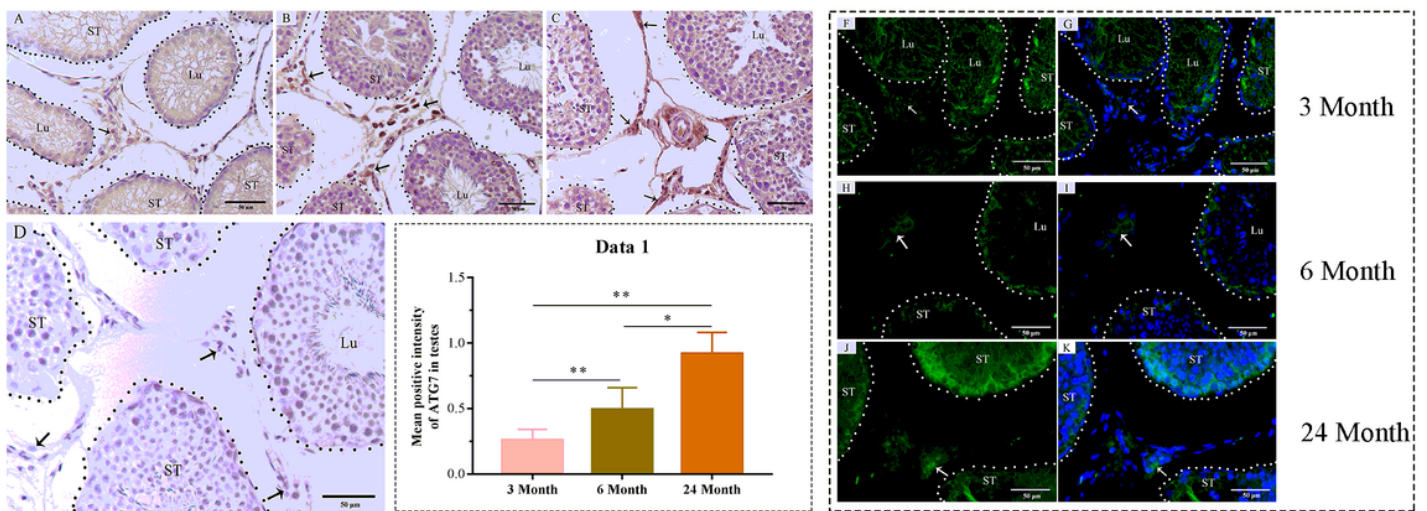


Figure 2

Ultrastructural analysis of LCs from the dairy goats at different development stages. Lipid droplets were observed in LCs at the juvenile (A), pubertal (B), and adult (C) stages by Oil red O staining. ST: seminiferous tubules; Lu: lumen; Black arrow: Leydig cells; Scale bar: A, B, and C = 50  $\mu$ m. Serum levels of LH (Data 1) and testosterone (Data 2) were analyzed using ELISA kit. The relative expressions of target genes involved in testosterone synthesis were detected using qPCR (Data 3). The average intensity of Oil red O staining in LCs based on Light micrographs (Data 4). Ultrastructural pictures of LCs at the juvenile (D), pubertal (E), and adult (F) stages. (G, H, and I) The higher magnification of the corresponding blue rectangle in upper panel, respectively. The histogram represents the quantification of nucleus diameter (Data 5), lipid droplets number within LC (Data 6), and lipid droplets size (Data 7), based on TEM pictures, respectively. N: nucleus; LD: lipid droplet; Mi: mitochondria; sER: smooth endoplasmic reticulum; Scale bar: D, E, and F = 2.0  $\mu$ m; G, H, and I = 1.0  $\mu$ m; Each value represents the mean  $\pm$  SEM, \* $p$  < 0.05, \*\* $p$  < 0.01.



### Figure 3

Lipophagy is not involved in testosterone synthesis in the LCs of dairy goats. Immunohistochemistry of ATG7 in the testes at the juvenile (A), pubertal (B), and adult (C) stages. D: negative control. Data 1: The mean positive intensity of ATG7 in testes. Each value represents the mean  $\pm$  SEM, \* $p < 0.05$ , \*\* $p < 0.01$ . ST: seminiferous tubules; Lu: lumen; Black arrow: Leydig cells; Scale bar = 50  $\mu\text{m}$ . Immunofluorescent analysis showed the expression of LC3 in the testes at the juvenile (F and G), pubertal (H and I), and adult (J and K) stages. White arrow: Leydig cells; Scale bar = 50  $\mu\text{m}$ . The colocalization of LC3 and lipid droplet (BODIPY 493/503) was analyzed using confocal microscopy in the testes at the juvenile (L, M and N), pubertal (O, P and Q), and adult (R, S and T) stages. White arrow: Leydig cells; Curved white arrow: there was no co-localization between LC3 and lipid droplet. Scale bar = 10  $\mu\text{m}$ . The ultrastructures of lipid droplets within Leydig cell at the juvenile (U), pubertal (V), and adult (W) stages. LD: lipid droplet; Mi: mitochondria; sER: smooth endoplasmic reticulum; Scale bar U, V, and W = 200 nm.

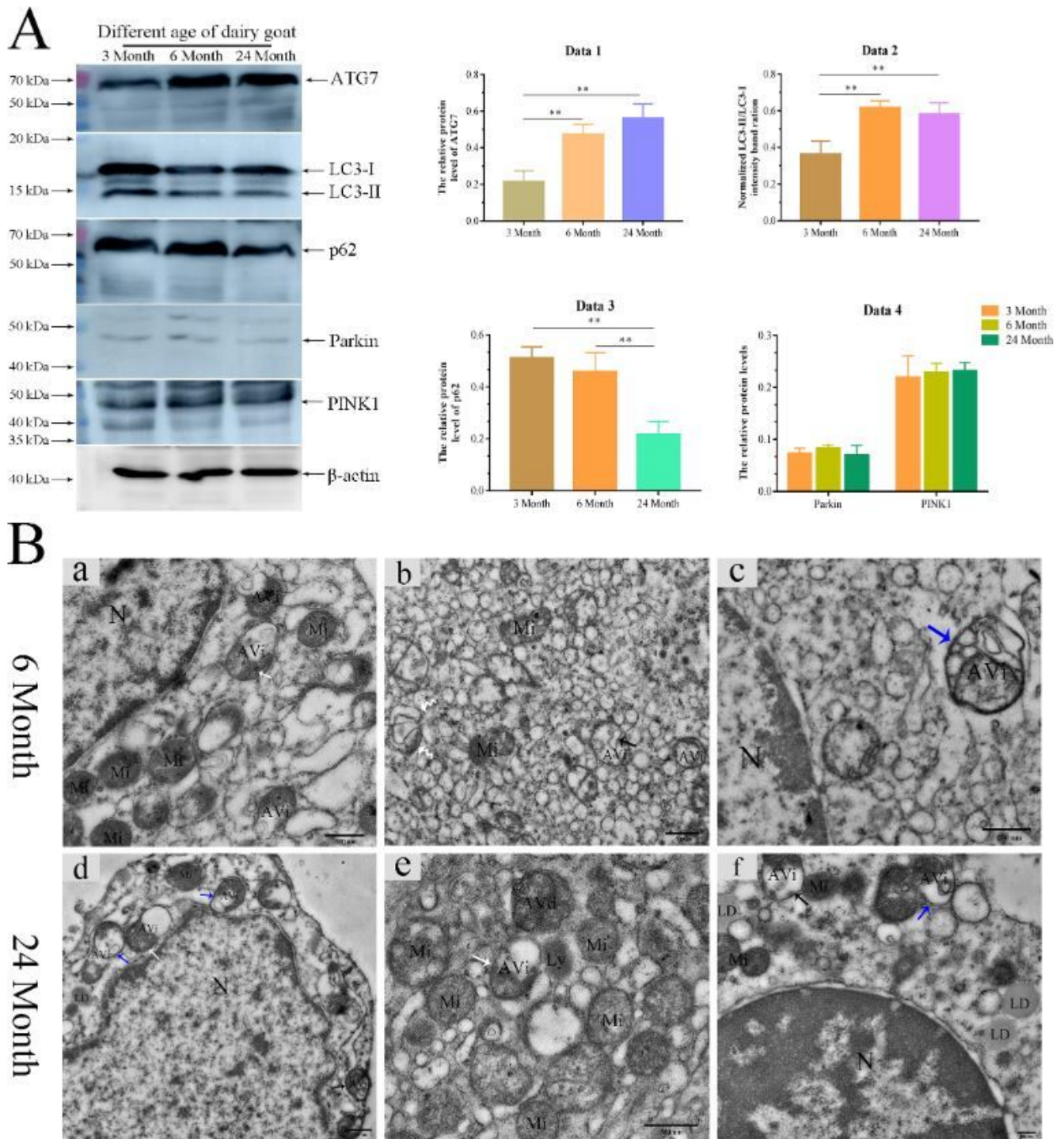


**Figure 4**

Macroautophagy might regulate testosterone synthesis in LCs of dairy goats. A: Western blot analysis was performed to measure the expression of proteins involved in autophagy.  $\beta$ -actin was utilized as a loading control. The histogram represents quantification of proteins levels of ATG7 (Data 1), LC3 (Data 2), p62 (Data 3), Parkin and PINK1 (Data 4), respectively. Each value represents the mean  $\pm$  SEM, \* $p < 0.05$ , \*\* $p < 0.01$ . B: Electron micrographs of autophagosomes within Leydig cells at the pubertal (a-c) and adult (d-f) stages. N: nucleus; Mi: mitochondria; LD: lipid droplet; White curved arrow: phagophore (pre-

autophagosome); AVi: autophagic vacuoles (autophagosome); AVd: autolysosome; Black arrow: autophagosomes mainly encase endoplasmic reticulum; White arrow: autophagosomes mainly encase mitochondria; Blue arrow: autophagosomes mainly encase mitochondria and endoplasmic reticulum; Scale bar a, b, d, and e = 500 nm; c and f = 200 nm.